Jpn J Radiol
DOI 10.1007/s11604-014-0377-y

ORIGINAL ARTICLE

Prediction of pancreatic anastomotic failure after pancreatic head resection using preoperative diffusion-weighted MR imaging

Noriyuki Miyamoto · Satoshi Yabusaki · Keita Sakamoto · Yasuka Kikuchi · Rie Mimura · Fumi Kato · Noriko Oyama-Manabe · Bunya Takahashi · Takeshi Soyama · Daisuke Abo · Yusuke Sakuhara · Kohsuke Kudo · Hiroki Shirato · Toru Nakamura · Takahiro Tsuchikawa · Keisuke Okamura · Satoshi Hirano

Received: 9 September 2014 / Accepted: 15 November 2014

Abstract
Purpose To determine whether the preoperative pancreatic apparent diffusion coefficient (ADC) can be used to predict the development of postoperative pancreatic anastomotic failure (PAF).
Materials and methods We retrospectively examined the cases of 79 patients who underwent pancreatic head resection between January 2010 and October 2013. The patients underwent 1.5-T MR imaging including diffusion-weighted imaging before surgery. The main pancreatic duct diameter (MPD), the pancreatic parenchymal thickness (PT), and the ADC of the pancreatic remnant parenchyma were measured. Two radiologists blinded to the patients' outcomes performed the measurements. The imaging parameters were compared between the patients who developed PAF and those who did not. The cut-off ADC for the development of PAF was calculated with a receiver operating characteristic analysis.
Results The imaging parameters were highly correlated between the two observers. The MPD and PT did not differ significantly among the patients. The mean pancreatic ADCs were significantly higher in the patients with PAF than in those without PAF. An ADC higher than 1.50×10^{-3} mm^2/s (Az = 0.719, observer-1) or 1.35×10^{-3} mm^2/s (Az = 0.752, observer-2) was optimal for predicting the development of postoperative PAF.
Conclusion Measuring the preoperative non-tumorous pancreatic ADC may be useful for the prediction of a postoperative PAF.

Keywords Pancreas · Post-operative anastomotic failure · MRI · Diffusion-weighted imaging · Apparent diffusion coefficient

Introduction

Postoperative pancreatic anastomotic failure (PAF) remains a significant problem after pancreatectomy because it may lead to deleterious secondary complications such as peripancreatic fluid collection, abscess formation, or bleeding from adjacent major vessels [1, 2]. It is generally reported that the incidence of clinically relevant PAF after pancreaticoduodenectomy is 7.6–36.4 % [3], in accord with the definition of PAF issued by the International Study Group of Pancreatic Fistula (ISGPF) [4].

The most frequently reported risk factors for PAF after pancreatectomy tend to be the anatomic features of a pancreatic remnant, such as a small pancreatic duct and a thick pancreas [3, 5]. The hardness of the pancreatic parenchyma is well known to be associated with the development of PAF after pancreatectomy [6]. Pancreatic fibrosis with decreased softness of the gland is thought to be associated with a decreased risk of PAF. A low rate of PAF in the presence of firm pancreatic parenchyma has been reported [7].

N. Miyamoto (✉) · S. Yabusaki · K. Sakamoto · Y. Kikuchi · R. Mimura · F. Kato · N. Oyama-Manabe · B. Takahashi · T. Soyama · D. Abo · Y. Sakuhara · K. Kudo
Department of Diagnostic and Interventional Radiology, Hokkaido University Graduate School of Medicine, N15 W7 Kita-ku, Sapporo, Hokkaido 060-8638, Japan
e-mail: nm-00@fg7.so-net.ne.jp

H. Shirato
Department of Radiation Medicine, Hokkaido University Graduate School of Medicine, Sapporo, Japan

T. Nakamura · T. Tsuchikawa · K. Okamura · S. Hirano
Department of Gastroenterological Surgery II, Hokkaido University Graduate School of Medicine, Sapporo, Japan

Published online: 11 December 2014

Several investigators have attempted to use dynamic computed tomography (CT) [6] or dynamic magnetic resonance (MR) imaging to demonstrate the degree of pancreatic fibrosis [8]. According to one report, the signal intensity ratio on unenhanced T1-weighted MR images has a diagnostic accuracy in prediction of PAF after pancreatectomy [9]. A recent study has shown promising results of the use of diffusion-weighted (DW) images in the diagnosis of the fibrosis [10]. Replacement of normal pancreatic parenchyma with fibrotic tissue cause decreased apparent diffusion coefficient (ADC) values [11]. This finding was attributed to the replacement of normal pancreatic parenchyma with fibrotic tissue and/or reduced exocrine function that may reduce the amount of diffusible tissue water and result in decreased ADCs [12]. Thus, we adopted ADC as a main MR parameter for predicting PAF. To our knowledge, the value of ADC in preoperative MR imaging has not been quantified as a tool for predicting postoperative PAF in a large patients.

In the present retrospective study, we investigated whether ADC measurement by preoperative DW MR imaging of the pancreas can be used as an accurate predictor of postoperative PAF in patients undergoing pancreatectomy.

Materials and methods

Patients

Approval for this retrospective study was obtained from the institutional review board of our hospital and the requirement for informed consent was waived. From January 2010 to October 2013, 104 consecutive patients underwent pancreatic head resection for pancreatic, periampullary and biliary diseases in our hospital. The criteria for inclusion in the present study were: pancreatic head resection, and a preoperative MR imaging and contrast-enhanced multidetector row CT (MDCT) examination performed at our hospital within the 3 months preceding the operation. Among the 104 patients, 93 consecutive patients underwent preoperative MR imaging and an MDCT examination. Fourteen of the 93 patients were excluded because it was difficult to assess the pancreatic tissue due to substantial artifact or atrophic pancreas on MR imaging. Thus, the remaining 79 patients comprised the patient series for this study. The median time between the MDCT examination and surgery was 14 days (1–140 days). The median time between the MRI and surgery was also 14 days (2–54 days).

Surgical procedures

A pancreatic head resection was achieved with a subtotal stomach-preserving pancreaticoduodenectomy (SSPPD) ($n = 59$), pancreaticoduodenectomy (PD) ($n = 9$), hepatopancreatoduodenectomy (HPD) ($n = 9$), or duodenum-preserving pancreas head resection (DPPHR) ($n = 2$) for various indications. Among the 79 patients, the final diagnosis was bile duct cancer in 36 patients, pancreatic cancer in 19 patients, duodenal cancer in 15 patients, intraductal papillary mucinous neoplasm in 4, endocrine tumor in 3, solid-pseudopapillary neoplasm of the pancreas in 1, and duodenal adenoma in 1. For reconstruction, pancreatojejunostomy ($n = 71$) or pancreatogastrostomy ($n = 8$) was performed. Although a pancreatojejunostomy is more commonly performed at our hospital, a pancreatogastrostomy is performed for the patients with severe comorbidities. The pancreatic stent tube was inserted into the remnant pancreatic duct. One closed-suction drain was routinely placed in proximity to the pancreatic anastomosis.

Definitions of pancreatic anastomotic failure

All patients were followed up by their team of surgeons, and evaluations of the amylase level of drainage fluid, serum amylase level, C-reactive protein, and white blood cell count were performed on days 1, 2, and 4 after surgery. Drains were removed when the drainage fluid did not show high amylase or signs of infection after postoperative days 3–6.

As noted earlier, PAF was defined and classified in accord with the ISGPS classification [4]. The ISGPS definition of PAF provides three levels of severity. Three different grades of postoperative PAF (grades A, B, and C) are defined according to the clinical effect on the patient's hospital course: grade A does not need specific treatment, grade B requires prolonged drainage or special medical treatment, and grade C requires invasive therapy [4]. In the present analyses, we combined grades B and C as the clinically relevant "PAF group," and we combined grade A and no PAF as the "no-PAF group" because it is well known that PAF grade A is not clinically relevant and therefore should not be considered as representing an important complication [6, 13].

Postoperative CT was not planned routinely but was carried out if the patient's clinical symptoms suggested an intra-abdominal inflammatory complication. In cases with drainage failure, percutaneous drainage was facilitated by ultrasound [14]. Major visceral arterial bleeding was managed by transcatheter arterial embolization (TAE) instead of emergency surgery [2, 15]. Percutaneous drainage and TAE were performed by four interventional radiologists (authors Y.S., D.A., T.S, and B.T., with 17, 15, 10, and 7 years of post-training experience in abdominal interventional radiology).

Preoperative MDCT technique

All patients were examined with a 320-detector-row CT instrument (Acquilion One; Toshiba Medical Systems, Tochigi, Japan). Unenhanced CT scans and enhanced CT scans in four-phase (arterial phase, pancreatic parenchymal phase, portal phase, and equilibrium phase) were obtained. An automatic bolus-tracking program (Real Prep, Toshiba Medical Systems) was used to determine the start timing of scanning for each phase after contrast material injection. The nonionic contrast material (560 mg of mean iodine per kg body weight) was delivered over 30 s. All images were reconstructed with a thickness of 2 mm. We used pancreatic parenchymal phase for pancreatic analysis.

Preoperative MR imaging technique

A 1.5-T superconducting system (Intera Achieva Nova Dual; Philips Medical Systems, Best, the Netherlands) with a six-channel torso array coil was used to perform MR imaging. We applied MR imaging with the contrast agent gadolinium ethoxybenzyl diethylenetriamine pentaacetic acid (Gd-EOB-DTPA) to investigate the presence of liver metastasis [16]. A negative oral contrast agent for MR imaging and antiperistaltics were not administered. The basic MR imaging with Gd-EOB-DTPA consisted of the following imaging sequences: breath-hold two-dimensional (2D) fat-suppressed axial T1-weighted fast field-echo imaging; respiratory-triggered 2D fat-suppressed axial T2-weighted turbo spin-echo imaging; respiratory-triggered 2D fat-suppressed axial heavy-T2-weighted turbo spin-echo imaging; free breathing 2D axial DW imaging with a single-shot echo-planer sequence; and breath-holding Gd-EOB-DTPA-enhanced imaging with fat-suppressed 3D spoiled fast field-echo sequence. Immediately after an intravenous administration of a bolus of Gd-EOB-DTPA (Primovist, Bayer Healthcare; 0.025 mmol/kg body weight), dynamic imaging in the arterial, portal venous and equilibrium phase was performed using a T1-weighted fat-suppressed sequence. Fifteen minutes postinjection, the T1-weighted fat-suppressed sequence was repeated.

In the present study, we analyzed two sequences (heavy-T2-weighted images and DW images) from basic MR imaging with Gd-EOB-DTPA protocols. ADC maps were generated from the DW imaging, and we calculated the ADC values of normal pancreatic parenchyma. The parameters used in this study are shown in Table 1.

Table 1 Sequence parameters used in MR imaging of the pancreas

Parameter	Heavy T2-weighted imaging	Diffusion-weighted imaging
Respiratory control	Respiratory triggered	Respiratory triggered
Sequence	2D single-shot TSE	2D single-shot EPI
Fat suppression	No	Yes
Repetition/echo time (ms)	2,000/200	2,000/66
Flip angle	90	90
b value (s/mm^3)	NA	0 and 1,000
Field of view (cm)	42 × 30	42 × 30
Matrix	256 × 256	128 × 90
No. of signals acquired	1	2
Sensitivity encoding factor	2	2
Section thickness (mm)	3	6
Intersection gap	0	0
No. of sections	58	29
Acquisition time	33 s	1 min 28 s

2D two dimensional, *TSE* turbo spin echo, *EPI* echo planar imaging
NA not applicable

Image analysis

The pancreatic parenchymal thickness (PT) and main pancreatic duct diameter (MPD) were measured by pancreatic parenchymal phase in MDCT and 3-mm axial heavy-T2-weighted MR images (Fig. 1). These were measured at the presumed pancreatic remnant site, which was determined with reference to the positional relationships with adjacent vessels (at the left side of the superior mesenteric vein). Duct dilatation was defined as MPD larger than 3 mm in diameter. The MPD was defined in a ventrodorsal direction. The PT was obtained in an approximately ventrodorsal direction vertical to the main pancreatic duct. We defined the MPD and PT as anatomical features.

The ADC values were measured by placing an ROI at two points in two segments of the pancreas (body and tail). The ROIs were placed in the pancreatic tissue unaffected by the tumor, distal to the left side of the superior mesenteric vein. The pancreas body and pancreas tail were divided at the left edge of the aorta according to the definition by the Union for International Cancer Control [17]. The ADC values were calculated for each ROI automatically by imager software (Vox Base, J-MAC, Sapporo, Japan).

A minimum area of 20 mm^2 of pancreatic parenchyma was required for ADC measurement, as this was the smallest ROI available with our measurement software, and it was the size used in our study. The largest possible oval ROI was placed making effort to avoid the pancreatic duct, cystic lesion, extrapancreatic structures, and artifacts. The mean value of the ROIs was computed for each patient.

Two radiologists (K.S., and S.Y., each with 8 years of post-training experience in interpreting body MR images) who had no knowledge of the patients' clinical information

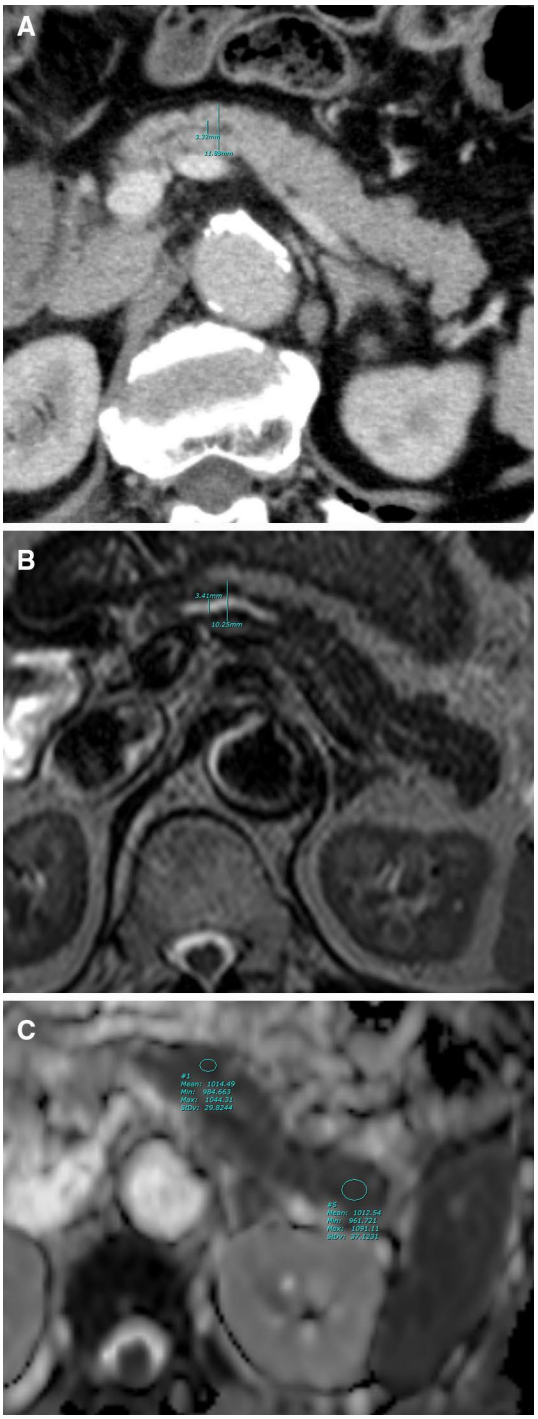

Fig. 1 Preoperative imaging of a patient with pancreatic head adenocarcinoma without subsequent PAF. **a** Contrast-enhanced MDCT: the main pancreatic duct diameter (MPD) was 3.32 mm and the pancreatic parenchymal thickness (PT) was 11.88 mm. **b** Heavy-T2-weighted image: MPD 3.41 mm, PT 10.25 mm. **c** ADC measured on an ADC map in the nontumoral pancreatic parenchyma (pancreatic body and tail). The averaged value of the two ROIs was 1.013×10^{-3} mm^2/s

performed all measurements by using a commercially available digital imaging and communications in medicine (DICOM) viewer (Vox Base).

Statistical analysis

We compared the PAF group and the no-PAF group using the Wilcoxon/Kruskal–Wallis test for continuous variables and chi-square tests for categorical variables. As for ADC, we evaluated the correlation between the severity of PAF and ADC. We evaluated the interobserver agreement by interclass correlation coefficient (ICC) using a two-way mixed-effects model for absolute agreement. ICC scores range from 0 to 1, representing a level of agreement as follows: $\leq$0.40 = poor to fair, 0.41–0.60 = moderate, 0.61–0.80 = substantial, 0.81–1.00 = almost perfect agreement [18].

We composed nonparametric receiver operating characteristic (ROC) curves for ADC values to assess the ability of ADC values to predict the development of PAF, and we calculated cutoff values, sensitivity, and specificity. We measured each model's accuracy by determining the area under curve (AUC) to evaluate how well the model distinguished patients with and without PAF. The data analyses were performed with commercially available software (JMP10, SAS institute, Cary, NC). In all comparisons, a $p < 0.05$ was considered to indicate a significant difference.

Results

Patient population and outcomes

The patients' characteristics and outcomes are summarized in Table 2. There were 54 men (68.5 %) and 25 women (31.5 %) with a mean age of 68.1 years (median 68 years; range 41–83 years). No postoperative mortality was observed. Based on the ISGPS classification, 14 patients (17.7 %) developed a clinically relevant PAF (seven grade B and grade C) and constituted the PAF group for this study. The no-PAF group consisted of the remaining 65 patients (no-PAF or grade A). Thirteen patients in the PAF group were managed by interventional radiology without operation (13 percutaneous drainage, seven percutaneous TAE). One PAF patient required hematoma evacuation, in addition to percutaneous drainage and TAE. No significant differences were observed between the PAF group and the no-PAF group in terms of age, sex, and type of operation. No-PAF occurred in the patients with pancreatic cancer, and only pancreatic cancer showed a significant difference

Table 2 Patient population and outcomes

	No-PAF ($n = 65$)	PAF ($n = 14$)	p value
Mean age, years (range)	67.6 (43–82)	70.6 (53–83)	0.215
Male:female	44:21	10:4	0.785
Diagnosis			
Bile duct cancer	26	10	0.065
Pancreatic cancer	19	0	0.048
Duodenal cancer	13	2	0.905
IPMN	3	1	0.779
pNET	2	1	0.961
Others (SPN, duodenal adenoma)	2	0	0.334
Operation			
SSPPD	49	10	0.976
PD	7	2	0.930
HPD	7	2	0.930
DPPHR	2	0	0.785

Values are mean with range or number of patients

IPMN intraductal papillary mucinous neoplasm, *pNET* pancreatic neuroendocrine tumor, *SPN* solid-pseudopapillary neoplasm, *SSPPD* subtotal stomach-preserving pancreaticoduodenectomy, *PD* pancreaticoduodenectomy, *HPD* hepatopancreaticoduodenectomy, *DPPHR* duodenum-preserving pancreas head resection

for the development of PAF ($p = 0.048$). No difference was seen between the two groups in terms of disease other than pancreatic cancer.

CT and MRI assessment

1. Interobserver variability

The interobserver agreement was substantial or almost perfect for each parameter: MPD in MDCT (ICC 0.940, $p < 0.01$), PT in MDCT (ICC 0.786, $p < 0.01$), MPD in MR imaging (ICC 0.969, $p < 0.01$), PT in MR imaging (ICC 0.762, $p < 0.01$), and ADC (ICC 0.871, $p < 0.01$).

2. Imaging parameters of the PAF and no-PAF groups

Among the imaging parameters, no considerable difference in MPD, PT, or duct dilatation was noted between the PAF and no-PAF groups (Table 3), but the pancreas ADC was significantly different between the two groups ($p = 0.011$ observer 1, $p = 0.003$ observer 2) (Fig. 2). In the PAF group, the ADCs of the pancreas ranged between 1.14×10^{-3} and 1.70×10^{-3} mm^2/s with a mean value of $1.45 \times 10^{-3} \pm 0.17 \times 10^{-3}$ mm^2/s (observer 1) and between 1.15×10^{-3} and 1.70×10^{-3} mm^2/s with a mean value of $1.52 \times 10^{-3} \pm 0.17 \times 10^{-3}$ mm^2/s (observer 2). In the no-PAF group, the ADCs of the pancreas ranged between 0.83×10^{-3} and 2.00×10^{-3} mm^2/s with a mean value of $1.30 \times 10^{-3} \pm 0.24 \times 10^{-3}$ mm^2/s (observer 1) and between 0.97×10^{-3} and 1.90×10^{-3} mm^2/s with a mean value of $1.34 \times 10^{-3} \pm 0.29 \times 10^{-3}$ mm^2/s (observer 2). The association of the PAF grade and ADC is presented in Table 4. In two observers, ADC varied significantly between no-PAF and PAF grade B, but not between PAF grade B and PAF grade C. In observer 1, ADC was higher in patients with PAF grade C compared with those with no-PAF, but the difference was not significant. In observer 2, ADC was significantly higher in patients with PAF grade C compared with those with no-PAF.

Table 3 Imaging assessment of remnant pancreas

Imaging parameter	No-PAF ($n = 65$)	PAF ($n = 14$)	p value
MDCT PT 1 (mm)	13.56 ± 3.90	15.37 ± 3.12	0.114
MDCT PT 2 (mm)	11.58 ± 4.60	15.27 ± 4.01	0.585
MDCT MPD 1 (mm)	4.21 ± 2.60	3.15 ± 1.71	0.057
MDCT MPD 2 (mm)	3.37 ± 2.48	2.94 ± 1.71	0.415
MDCT duct dilatation 1 > 3 mm [n (%)]	37 (57 %)	5 (36 %)	0.150
MDCT duct dilatation 2 > 3 mm [n (%)]	28 (43 %)	5 (37 %)	0.612
MR PT 1 (mm)	14.26 ± 3.88	15.00 ± 3.26	0.504
MR PT 2 (mm)	15.26 ± 3.42	15.55 ± 3.65	0.928
MR duct dilatation 1 > 3 mm [n (%)]	34 (52 %)	6 (43 %)	0.521
MR duct dilatation 2 > 3 mm [n (%)]	31 (48 %)	7 (50 %)	0.875
MR MPD 1 (mm)	4.18 ± 2.54	3.15 ± 1.19	0.869
MR MPD 2 (mm)	3.74 ± 2.17	3.29 ± 2.35	0.504
MR ADC 1 ($\times 10^{-3}$ mm^2/s)	1.30 ± 0.24	1.45 ± 0.17	0.011
MR ADC 2 ($\times 10^{-3}$ mm^2/s)	1.34 ± 0.29	1.52 ± 0.17	0.003

Data are mean ± standard deviation

PT pancreatic parenchymal thickness, *MPD* main pancreatic duct diameter, *1* observer 1, *2* observer 2

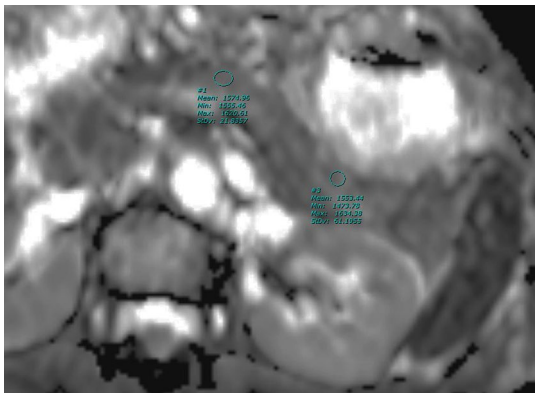

Fig. 2 Bile duct cancer in a 72-year-old woman who subsequently developed postoperative PAF. The averaged ADC value of the nontumoral pancreatic parenchyma was 1.575×10^{-3} mm^2/s

Table 4 Correlation between PAF grade and ADC

	No-PAF	PAF B	PAF C	*p* value			
				All groups	No-PAF versus PAF B	No-PAF versus PAF C	PAF B versus PAF C
ADC1 ($\times 10^{-3}$ mm^2/s)	1.30 ± 0.24	1.52 ± 0.17	1.38 ± 0.15	0.022	0.012	0.210	0.125
ADC2 ($\times 10^{-3}$ mm^2/s)	1.34 ± 0.29	1.52 ± 0.20	1.52 ± 0.15	0.013	0.022	0.042	0.610

Data are mean ± standard deviation

1 observer 1, *2* observer 2, *B* grade B, *C* grade C

Table 5 Most accurate ADC threshold levels for PAF versus no PAF

	Area under the curve	Best cut-off ADC	Sensitivity (%)	Specificity (%)
Observer 1	0.719	1.354	78.6	67.7
Observer 2	0.752	1.495	78.6	78.5

3. ADC threshold levels for PAF

We calculated the cut-off values for the ADC of the pancreas with respect to the presence of a PAF (Table 5). The ROC analysis revealed that the cut-off value of 1.354 (AUC = 0.719) had 78.6 % sensitivity and 67.7 % specificity (observer 1), and that the cut-off value of 1.495 (AUC = 0.752) had 78.6 % sensitivity and 78.5 % specificity (observer 2) for the development of PAF.

Discussion

PAF is a leading cause of morbidity and mortality after PD. To achieve acceptable outcomes, it is necessary to perform an accurate preoperative assessment of the PAF risk as well as appropriate surgical techniques and perioperative management, especially for high-risk cases. Factors underlying the development of PAF have been studied [19, 20]. The most widely recognized risk factor for the development of PAF is intraoperative soft texture of the remnant pancreas [3, 6, 21]. For example, Yeo et al. [22] reported no-PAF in their patients with a firm pancreas compared to a 25 % PAF rate in the patients with a soft pancreas. A firm pancreas is thought to decrease the softness of the gland [21, 23]. Pancreatic firmness is mainly affected by underlying pancreatic pathology such as chronic pancreatitis [24]. Thus, the assessment of preoperative features of pancreatic parenchymal texture that are highly linked to the occurrence of PAF is a promising area of investigation.

It was shown that CT or MR imaging can detect fibrotic change in the liver and pancreas [11, 25]. Tajima et al. [8] used dynamic contrast-enhanced MR with Gd-DTPA to assess fibrosis in the remnant pancreas after PD. They noted that the time-signal intensity curve (TIC) in normal pancreas showed a rapid rise followed by a rapid decline, whereas the TIC in fibrotic pancreas showed a slow rise to a peak followed by a slow decline or plateau. They reported that patients with a rapid rise in the TIC profile more frequently developed PAF than patients with a slowly rising TIC profile (93 vs 52 %, $p = 0.006$), and they concluded that the TIC obtained from MR is a reliable indicator for fibrosis in the remnant pancreas. In this study, we used Gd-EOB-DTPA as a contrast agent. In view of enhancement effects, the standard dose of Gd-EOB-DTPA is 25 % compared with Gd-DTPA (0.025 mmol/kg of Gd-EOB-DTPA vs 0.1 mmol/kg of Gd-DTPA). The enhancement effect of abdominal solid organs in dynamic contrast-enhanced MR imaging with Gd-EOB-DTPA is significantly weaker than with that of Gd-DTPA [26]. Thus, we did not evaluate dynamic-enhanced MR imaging.

Hashimoto and Traverso [20] analyzed the pancreatic late/early enhancement ratio (L/E ratio), which is the ratio of pancreatic enhancement in the late phase of CT to the enhancement during the early phase, and they found that the histologic degree of pancreatic fibrosis showed a good correlation with the L/E ratio. They concluded that an L/E ratio ≤1.0 is correlated with a soft pancreas, and they reported that their patients with an L/E ratio ≤1.0 developed PAF significantly more frequently than the patients with an L/E ratio >1.0 (65 vs 10 %, $p < 0.001$).

The pancreatic firmness may be influenced by pancreatic fat infiltration [27]. Using dual-gradient MR imaging, Lee et al. [23] found that a relative signal intensity decrease was correlated with the pancreatic fat content and predicted the development of PAF. They concluded that the measurement of fat content by MR imaging allowed them to predict the occurrence of PAF with 72.5 % sensitivity and 75.9 % specificity. Their results were almost the same as ours.

DW imaging measures changes in the microscopic diffusion of water. In the liver, fibrosis and cirrhosis have been shown to reduce diffusion [28]. DW imaging has also been used for the assessment of chronic pancreatitis [29]. The ADC values for patients with pancreatitis are lower than those found for patients with normal pancreases [11, 25]. This finding is attributed to the replacement of normal

pancreatic parenchyma with fibrous tissue and/or reduced exocrine function that may reduce the amount of diffusive tissue water and result in decreased ADCs [11]. Watanabe et al. [9] showed that the expression of activated pancreatic stellate cells was correlated with the progression of fibrosis. They documented that the ADC values of pancreatic parenchyma were highly correlated with the expression of activated pancreatic stellate cells.

However, no data were available to date that compared the relationships between the ADC values and postoperative PAF development in a large patient series. Here we observed significantly higher pancreatic ADC values in the patients with PAF compared to those with no-PAF. According to previous studies [9, 12], the high ADC values may reflect the soft, nonfibrotic pancreatic remnant. Although there was a significant overlap in ADCs between our patients with PAF and the patients without PAF, the most discriminating ADC cut-off value setting on the ROC yielded sufficiently high sensitivity and specificity for the prediction of PAF. Accordingly, we believe that the ADC measurement may be useful for the prediction of the occurrence of PAF, and for preoperative risk stratification and postoperative patient management.

Pancreatic duct size and PT are recognized risk factors for PAF [3, 6, 20]. In our present study, however, these anatomical features were not significant predictors of the development of PAF. The reason for this discrepancy might be the differences in study populations. In our study, the percentage of patients with pancreatic cancer was relatively low (19 of 79 patients; 24.1 %). Generally, pancreatic ductal dilatation and pancreatic atrophy are detected in many cases of pancreatic head cancer.

Our study has several limitations. First, this was a retrospective study, and it relied on clinical evaluations for the diagnosis of PAF, in which the intraoperative and histopathologic findings of the remnant pancreas were lacking. Thus, our results should be considered preliminary. A prospective study with comparisons of ADC values and histopathological findings is needed. Second, we adopted ADC as a main MR parameter for predicting PAF; however, it is necessary to determine which imaging parameters, such as unenhanced T1-weighted image, chemical shift gradient-echo image, and dynamic contrast-enhanced study, are the most useful for PAF prediction. Third, the percentage of the patients having duct dilatation was low compared with previous reports [3, 6]. Thus, it is not clear whether our ADC results may be applied in the patients with pancreatic duct dilatation and pancreatic atrophy. Fourth, ADC measurements are unavoidably subject to error, particularly in body imaging applications, due to both a low signal-to-noise ratio and artifacts caused by physiologic motion and magnetic susceptibility. Peristalsis and respiratory motion results in blurring. Susceptibility artifacts from the presence of bowel gas may be marked on DW imaging. We used multiple signal acquisition rather than a breath-hold technique, to improve the patients' tolerance of the complex protocol. Therefore, ADC measurement could not be performed in 14 patients (15.4 %), and these missing data could have affected the results. In particular, measurements often could not be made in the patients with severe pancreatic atrophy. This may induce a bias; however, the clinical importance of this is mitigated since a severely atrophic pancreas is thought to be linked to a decreased incidence of PAF. To optimize imaging, several procedures may be helpful. Prior to imaging, oral negative contrast agents can eliminate the signals from the gastrointestinal system [30]; antiperistaltics to reduce blurring artifacts may also be beneficial. Fifth, ADC measurements also have a major limitation for quantitative evaluation. Braithwaite et al. demonstrated the overall coefficient of variation value as 14 % in abdominal DW imaging, and they stated that a change in ADC values less than approx. 27 % will not be clinically detectable with confidence with one acquisition in a single individual [31]. To use the ADC as a qualitative tool, it is necessary to perform repeated measurements carefully.

In conclusion, our results suggest that an elevated ADC value obtained with DW imaging is a risk factor for the development of PAF. We believe that ADC measurement could serve as a noninvasive biomarker to efficiently perform preoperative risk stratification, patient counseling, and pre- and postoperative patient management. A large cohort study is called for to test our present findings.

Acknowledgments We obtained valuable advice from Dr. Koji Oba (Translational Research and Clinical Trial Center, Hokkaido University Hospital).

Conflict of interest We have no conflict of interest.

References

1. Wellner UF, Kayser G, Lapshyn H, Sick O, Makowiec F, Hoppner J, et al. A simple scoring system based on clinical factors related to pancreatic texture predicts postoperative pancreatic fistula preoperatively. HPB Off J Int Hepato Pancreato Biliary Assoc. 2010;12(10):696–702.
2. Miyamoto N, Kodama Y, Endo H, Shimizu T, Miyasaka K. Hepatic artery embolization for postoperative hemorrhage in upper abdominal surgery. Abdom Imaging. 2003;28(3):347–53.
3. Sugimoto M, Takahashi S, Gotohda N, Kato Y, Kinoshita T, Shibasaki H, et al. Schematic pancreatic configuration: a risk assessment for postoperative pancreatic fistula after pancreaticoduodenectomy. J Gastrointest Surg Off J Soc Surg Aliment Tract. 2013;17(10):1744–51.
4. Bassi C, Dervenis C, Butturini G, Fingerhut A, Yeo C, Izbicki J, et al. Postoperative pancreatic fistula: an international study group (ISGPF) definition. Surgery. 2005;138(1):8–13.

5. de Castro SM, Busch OR, van Gulik TM, Obertop H, Gouma DJ. Incidence and management of pancreatic leakage after pancreatoduodenectomy. Br J Surg. 2005;92(9):1117–23.
6. Hashimoto Y, Sclabas GM, Takahashi N, Kirihara Y, Smyrk TC, Huebner M, et al. Dual-phase computed tomography for assessment of pancreatic fibrosis and anastomotic failure risk following pancreatoduodenectomy. J Gastrointest Surg Off J Soc Surg Aliment Tract. 2011;15(12):2193–204.
7. Lin JW, Cameron JL, Yeo CJ, Riall TS, Lillemoe KD. Risk factors and outcomes in postpancreaticoduodenectomy pancreaticocutaneous fistula. J Gastrointest Surg Off J Soc Surg Aliment Tract. 2004;8(8):951–9.
8. Tajima Y, Kuroki T, Tsutsumi R, Fukuda K, Kitasato A, Adachi T, et al. Risk factors for pancreatic anastomotic leakage: the significance of preoperative dynamic magnetic resonance imaging of the pancreas as a predictor of leakage. J Am Coll Surg. 2006;202(5):723–31.
9. Watanabe H, Kanematsu M, Tanaka K, Osada S, Tomita H, Hara A, et al. Fibrosis and postoperative fistula of the pancreas: correlation with MR imaging findings—preliminary results. Radiology. 2014;270(3):791–9.
10. Cece H, Ercan A, Yildiz S, Karakas E, Karakas O, Boyaci FN, et al. The use of DWI to assess spleen and liver quantitative ADC changes in the detection of liver fibrosis stages in chronic viral hepatitis. Eur J Radiol. 2013;82(8):e307–12.
11. Akisik MF, Aisen AM, Sandrasegaran K, Jennings SG, Lin C, Sherman S, et al. Assessment of chronic pancreatitis: utility of diffusion-weighted MR imaging with secretin enhancement. Radiology. 2009;250(1):103–9.
12. Balci NC, Momtahen AJ, Akduman EI, Alkaade S, Bilgin M, Burton FR. Diffusion-weighted MRI of the pancreas: correlation with secretin endoscopic pancreatic function test (ePFT). Acad Radiol. 2008;15(10):1264–8.
13. Roberts KJ, Hodson J, Mehrzad H, Marudanayagam R, Sutcliffe RP, Muiesan P, et al. A preoperative predictive score of pancreatic fistula following pancreatoduodenectomy. HPB Off J Int Hepato Pancreato Biliary Assoc. 2014;16(7):620–8.
14. Zink SI, Soloff EV, White RR, Clary BM, Tyler DS, Pappas TN, et al. Pancreaticoduodenectomy: frequency and outcome of postoperative imaging-guided percutaneous drainage. Abdom Imaging. 2009;34(6):767–71.
15. Schafer M, Heinrich S, Pfammatter T, Clavien PA. Management of delayed major visceral arterial bleeding after pancreatic surgery. HPB Off J Int Hepato Pancreato Biliary Assoc. 2011;13(2):132–8.
16. Kim A, Lee CH, Kim BH, Lee J, Choi JW, Park YS, et al. Gadoxetic acid-enhanced 3.0T MRI for the evaluation of hepatic metastasis from colorectal cancer: metastasis is not always seen as a "defect" on the hepatobiliary phase. Eur J Radiol. 2012;81(12):3998–4004.
17. Adsay NV, Bagci P, Tajiri T, Oliva I, Ohike N, Balci S, et al. Pathologic staging of pancreatic, ampullary, biliary, and gallbladder cancers: pitfalls and practical limitations of the current AJCC/UICC TNM staging system and opportunities for improvement. Semin Diagn Pathol. 2012;29(3):127–41.
18. Desmet VJ, Gerber M, Hoofnagle JH, Manns M, Scheuer PJ. Classification of chronic hepatitis: diagnosis, grading and staging. Hepatology (Baltimore, Md). 1994;19(6):1513–20.
19. Farnell MB, Pearson RK, Sarr MG, DiMagno EP, Burgart LJ, Dahl TR, et al. A prospective randomized trial comparing standard pancreatoduodenectomy with pancreatoduodenectomy with extended lymphadenectomy in resectable pancreatic head adenocarcinoma. Surgery. 2005;138(4):618–28; discussion 28–30.
20. Hashimoto Y, Traverso LW. Incidence of pancreatic anastomotic failure and delayed gastric emptying after pancreatoduodenectomy in 507 consecutive patients: use of a web-based calculator to improve homogeneity of definition. Surgery. 2010;147(4):503–15.
21. Dinter DJ, Aramin N, Weiss C, Singer C, Weisser G, Schoenberg SO, et al. Prediction of anastomotic leakage after pancreatic head resections by dynamic magnetic resonance imaging (dMRI). J Gastrointest Surg Off J Soc Surg Aliment Tract. 2009;13(4):735–44.
22. Yeo CJ, Cameron JL, Lillemoe KD, Sauter PK, Coleman J, Sohn TA, et al. Does prophylactic octreotide decrease the rates of pancreatic fistula and other complications after pancreaticoduodenectomy? Results of a prospective randomized placebo-controlled trial. Ann Surg. 2000;232(3):419–29.
23. Lee SE, Jang JY, Lim CS, Kang MJ, Kim SH, Kim MA, et al. Measurement of pancreatic fat by magnetic resonance imaging: predicting the occurrence of pancreatic fistula after pancreatoduodenectomy. Ann Surg. 2010;251(5):932–6.
24. Yeo CJ, Cameron JL, Sohn TA, Lillemoe KD, Pitt HA, Talamini MA, et al. Six hundred fifty consecutive pancreaticoduodenectomies in the 1990s: pathology, complications, and outcomes. Ann Surg. 1997;226(3):248–57.
25. Ronot M, Asselah T, Paradis V, Michoux N, Dorvillius M, Baron G, et al. Liver fibrosis in chronic hepatitis C virus infection: differentiating minimal from intermediate fibrosis with perfusion CT. Radiology. 2010;256(1):135–42.
26. Tamada T, Ito K, Sone T, Yamamoto A, Yoshida K, Kakuba K, et al. Dynamic contrast-enhanced magnetic resonance imaging of abdominal solid organ and major vessel: comparison of enhancement effect between Gd-EOB-DTPA and Gd-DTPA. J Magn Reson Imaging JMRI. 2009;29(3):636–40.
27. Mathur A, Pitt HA, Marine M, Saxena R, Schmidt CM, Howard TJ, et al. Fatty pancreas: a factor in postoperative pancreatic fistula. Ann Surg. 2007;246(6):1058–64.
28. Taouli B, Tolia AJ, Losada M, Babb JS, Chan ES, Bannan MA, et al. Diffusion-weighted MRI for quantification of liver fibrosis: preliminary experience. AJR Am J Roentgenol. 2007;189(4):799–806.
29. Balci C. MRI assessment of chronic pancreatitis. Diagn Interv Radiol. 2011;17(3):249–54.
30. Morita S, Ueno E, Masukawa A, Suzuki K, Fujimura M, Hirabayashi N, et al. Prospective comparative study of negative oral contrast agents for magnetic resonance cholangiopancreatography. Jpn J Radiol. 2010;28(2):117–22.
31. Braithwaite AC, Dale BM, Boll DT, Merkle EM. Short- and midterm reproducibility of apparent diffusion coefficient measurements at 3.0-T diffusion-weighted imaging of the abdomen. Radiology. 2009;250(2):459–65.